Theoretical and Mathematical Physics, **203**(2): 700–708 (2020)

FIELDS OF A RELATIVISTIC BEAM OF CHARGED PARTICLES BETWEEN PARALLEL PLANES: EXACT TWO-DIMENSIONAL SOLUTIONS OBTAINED BY THE METHOD OF IMAGES

B. B. Levchenko*

We calculate exact two-dimensional analytic expressions for the electric and magnetic fields and their potentials generated by a linear beam of relativistic charged particles between infinite ideally conducting planes and ferromagnetic poles. We use the method of summing an infinite sequence of fields of linear image charges and image currents to obtain solutions and also calculate the density distribution of the electric charge on the conductor surface induced by the charged particle beam. We obtain new formulas for the linear approximation of the fields near the beam and discuss the mathematical features of the exact solutions and the applicability constraints for the linear approximations.

Keywords: charged-beam electromagnetic field, ideal conductor, parallel infinite planes, exact solution, method of images

DOI: 10.1134/S0040577920050116

1. Introduction

The external electric field $\mathbf{E}$ and the magnetic induction $\mathbf{B}$ of a beam of relativistic charged particles with a uniform linear density and a circular cross section in a vacuum are described by the expressions (see Chap. 18.2.4 in [1] and also [2])

$$\mathbf{E} = \frac{2\kappa\lambda}{r}\frac{\mathbf{r}}{r}, \qquad \mathbf{B} = \frac{1}{c}\boldsymbol{\beta}\times\mathbf{E}, \tag{1}$$

where $\kappa = 1/4\pi\epsilon_0$, λ denotes the linear density of the beam with the sign of the particle charge taken into account, and $\boldsymbol{\beta} = \mathbf{v}/c$ is the velocity vector of particles in the beam normalized by the speed of light c. The radius vector $\mathbf{r}$ is perpendicular to the beam velocity vector.

If the beam is surrounded by conducting surfaces and magnets (as in charged-particle accelerators), then the fields around the beam change.[1] These changes can be taken into account by a comparatively simple technique developed by William Thomson (Lord Kelvin) [3] and described in detail in Maxwell's treatise [4], which is called the method of mirror charges and currents or the method of images. The one-dimensional field projections E_y and B_x were first calculated by the method of images in [5], where the problem of the fields $\mathbf{E}$ generated by a cylindrical beam between parallel ideally conducting planes and of the fields $\mathbf{B}$ between parallel ferromagnetic poles was considered. The planes of both types are parallel and

*Skobeltsyn Institute of Nuclear Physics, Lomonosov Moscow State University, Moscow, Russia, e-mail: levtchen@mail.desy.de.

[1] In what follows, we consider the fields generated by the beam itself, i.e., the (direct) proper fields (with the subscript dir) and the fields of induced charges and currents (with the subscript im).

Translated from Teoreticheskaya i Matematicheskaya Fizika, Vol. 203, No. 2, pp. 311–320, May, 2020. Received October 11, 2019. Revised November 26, 2019. Accepted January 28, 2020.

symmetric with respect to the coordinate plane (x, z). An infinite sequence of fields of image charges and image currents was summed in the approximation respectively linear in y and $\bar{y}$, the coordinate $(0, y)$ of the field observation point on the axis y, and the value of the beam displacement from the origin.

As a result, additional induced fields arise near the beam [5],

$$\mathrm{E}_{y,\mathrm{im}}(y, \bar{y}) = \frac{4\kappa\lambda}{h}\epsilon_1(\delta + 2\bar{\delta}), \qquad \mathrm{B}_{x,\mathrm{im}}(y, \bar{y}) = \frac{2\kappa\lambda\beta}{gc}\epsilon_2(2\eta + \bar{\eta}). \tag{2}$$

The coefficients $\epsilon_1 = \pi^2/48$ and $\epsilon_2 = \pi^2/24$ are called the Laslett form factors for the respective infinite parallel conducting planes and magnetic poles. The variables $\delta = y/h$, $\bar{\delta} = \bar{y}/h$, $\eta = y/g$, and $\bar{\eta} = \bar{y}/g$ correspond to the variables y and $\bar{y}$ normalized by the half-distance h between the conducting planes and by the half-distance g between the magnetic poles. Precisely this (incomplete) linear approximation[2] is given in textbooks and reference manuals (see, e.g., [1], [6]).

The applicability constraints for the linear approximation are not satisfied in the cases where the field observation point y is located far from the beam and where the beam center $\bar{y}$ itself is displaced far toward the conducting surface. We presented the exact solution of this one-dimensional problem obtained by the method of images in [7],

$$\mathrm{E}_{y,\mathrm{im}}(\delta, \bar{\delta}) = \frac{4\kappa\lambda}{h}\Lambda(\delta, \bar{\delta}), \qquad \mathrm{B}_{x,\mathrm{im}}(\eta, \bar{\eta}) = \frac{4\kappa\lambda\beta}{gc}H(\eta, \bar{\eta}), \tag{3}$$

where the structure functions of the fields become

$$\begin{aligned}
\Lambda(\delta, \bar{\delta}) &= \frac{1}{2}\left\{\frac{\pi}{4}\tan\left[\frac{\pi}{4}(\delta + \bar{\delta})\right] + \frac{\pi}{4}\cot\left[\frac{\pi}{4}(\delta - \bar{\delta})\right] - \frac{1}{\delta - \bar{\delta}}\right\}, \\
H(\eta, \bar{\eta}) &= \frac{1}{2}\left\{\frac{\pi}{4}\tan\left[\frac{\pi}{4}(\eta + \bar{\eta})\right] - \frac{\pi}{4}\cot\left[\frac{\pi}{4}(\eta - \bar{\eta})\right] + \frac{1}{\eta - \bar{\eta}}\right\}.
\end{aligned} \tag{4}$$

Expanding the trigonometric functions in series, we can obtain both approximations (2) and the complete linear approximations in y including the generalized form factors $\epsilon_1(\bar{\delta})$ and $\epsilon_1(\bar{\eta})$, which hold for arbitrary $\bar{\delta}$ and $\bar{\eta}$ [2]. The complete linear approximation is important for studying the dynamics of both the particles near the beam and the beam itself in the case of significant deviations from the middle plane.

Representing the accelerator vacuum chamber and the poles of magnets as infinite parallel plates is a very useful mathematical abstraction. But all devices in real accelerators have finite dimensions. At the same time, some devices contain elements whose structure is based on the use of parallel conducting and ferromagnetic plane surfaces. In circular accelerators such as the Large Hadron Collider (LHC), the plane parallel surfaces are a part of different collimators and normal dipole magnets (orbit dividers and correctors). The LHC contains more than a hundred collimators (see Table 5-1 in [8]). The construction of the infrastructure for an upgraded version of the LHC with high luminosity (HL-LHC) has started [8]. As a rule, the width of the collimator jaws is nearly 90 mm, and the width of poles in the dipole magnets is 60 mm. The transverse size of the beam in the HL-LHC is at most 200 μm, which is much less than the width of those surfaces. Therefore, the representation of collimators and dipole poles as infinite parallel plates is a good approximation and justifies the applicability of the formulas obtained in applied calculations.

The transverse profile of the beam in the accelerator is formed not only by the magnetic system but also by collimators absorbing the beam halo and protecting the other parts of the accelerator if the beam is unstable. The collimator surfaces are manufactured of electrically conducting alloys resistant to the

[2]The complete linear approximation is here understood as an expression linear in y but summed over all orders of $\bar{y}$.

temperature and impact mechanical loads. The beam of relativistic charged particles is the source of a strong electric field. Precisely in the collimator, the beam is closest to the electrically conducting surfaces. As a consequence of these factors, a field emission of electrons occurs on the collimator surface [9]. Entering the accelerator channel, these electrons generate a whole chain of processes affecting the stability of the high-energy beam. Electrons accelerated by the electric field of the beam begin to collide with the walls of the vacuum system, knock out additional electrons, and radiate bremsstrahlung photons, thus initiating a cascade multiplication of the number of electrons [10].

To calculate the particle trajectories in the beam halo or the evolution of electrons emitted from the collimator planes, we must know the two-dimensional distribution of fields in the gap between the planes. Below, we present exact two-dimensional solutions for the distribution of the fields **E** and **B**.

2. Electric fields of image charges

We now calculate the field **E** in the gap between ideally conducting parallel planes when the particle beam moves parallel to the plates.

The z axis of the Cartesian coordinate system (x, y, z) is directed along the velocity vector of the particle beam, and the y axis is perpendicular to the conducting plates. The plates themselves are located at the distance $y = \pm h$ from the origin. The x axis is perpendicular to the beam and located in the middle plane between the plates. We assume that the charge of the beam particles is positive (e.g., this can be a beam of protons or ions). Our problem is two-dimensional and static by construction, and it is hence only necessary to calculate the field components in the plane (x, y). We displace the beam center to a point $(\bar{x}, \bar{y})$ for more generality.

The boundary condition on the x-component of the electric field on the surface of ideally conducting plates (equipotential surfaces) $\mathrm{E}_x(x, \pm h) = 0$ is satisfied if the image charges change sign from image to image.

A test charged particle located at the point (x, y) is under the action of both the direct field of the source charge λ_0 and the field of all image charges $\lambda_{\pm i}$ [1], [6], as is shown in Fig. 1. For example, the charges[3] λ_1 and λ_{-1} are generated by λ_0 in reflecting from the respective planes $+h$ and $-h$, and the charges λ_2 and λ_{-2} are generated by the charges λ_{-1} and λ_1 in reflecting from the respective plates $+h$ and $-h$, and so on. Figure 1 permits easily calculating the y coordinates of all charges. Hence, the differences of the y coordinates between $\lambda_{\pm k}$ and the observation point y are equal to $d_{\pm k} = 2kh \mp y_+$ for odd images $(k = 1, 3, 5, \dots)$, and the differences of the y coordinates between $\lambda_{\pm m}$ and the observation point y are equal to $d_{\pm m} = 2mh \mp y_-$ for even images $(m = 2, 4, 6, \dots)$. Here, $y_+ = y + \bar{y}$ and $y_- = y - \bar{y}$.

The one-dimensional problem could be solved successfully because the distance between the field points is determined by both the simple difference of coordinates and the need to sum a series of elementary fractions [7]. The distance in the two-dimensional problem is already determined by a polynomial function. Passing to the potential significantly simplifies solving the electrostatics problems.

In the complex-z plane $(z = x + iy)$, we introduce the field $\mathrm{E}(z) = -\partial \mathrm{U}/\partial z$. If the complex potential of the beam with the linear charge density λ is defined as $\mathrm{U}(z - \bar{z}) = -2\kappa\lambda \log(z - \bar{z})$, then the complex field of such a beam is $\mathrm{E}(z) = 2\kappa\lambda/(z - \bar{z})$, where $\bar{z} = \bar{x} + i\bar{y}$. Hence, the proper field of the beam in the component representation becomes

$$\mathrm{E}_{\mathrm{dir}}(z) = \frac{2\kappa\lambda}{|r - \bar{r}|} \cdot \frac{x - \bar{x}}{|r - \bar{r}|} - i\frac{2\kappa\lambda}{|r - \bar{r}|} \cdot \frac{y - \bar{y}}{|r - \bar{r}|} = \mathrm{E}_{x,\mathrm{dir}} - i\mathrm{E}_{y,\mathrm{dir}}. \tag{5}$$

[3] In what follows, we write "charge" instead of "image charge" for brevity.

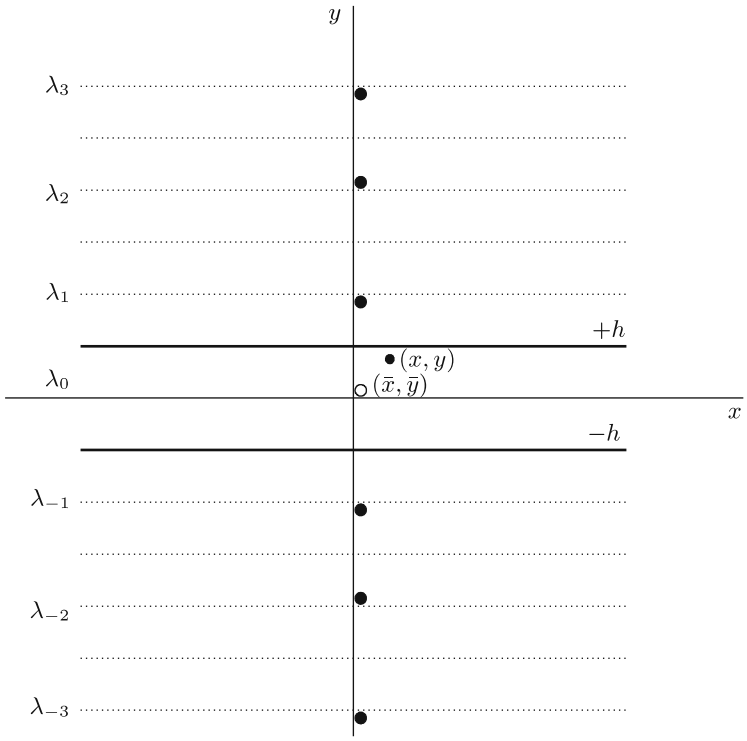

Fig. 1. Electric field at the point (x, y) between the conducting planes $y = \pm h$ is created by the source charge λ_0 from the point $(\bar{x}, \bar{y})$ (direct field) and the sequence of image charges $\lambda_{\pm i}$ located at the points $(\bar{x}, d_{\pm k})$ and $(\bar{x}, d_{\pm m})$.

We construct the sum of potentials of the first-level images λ_1 and λ_{-1} (Fig. 1),

$$\begin{aligned} \mathrm{U}_1 &= -2\kappa\lambda[(-1)\log(z - z_1) + (-1)\log(z - z_{-1})] = \\ &= 2\kappa\lambda\{\log[x - \bar{x} + i(y_+ - 2h)] + \log[x - \bar{x} + i(y_+ + 2h)]\} = \\ &= 2\kappa\lambda\log[\hat{z}_+^2 + (2h)^2], \end{aligned} \tag{6}$$

where $\hat{z}_+ = x - \bar{x} + iy_+$. For an arbitrary odd $k = 2n + 1$, we have

$$\mathrm{U}_k = 2\kappa\lambda\log[\hat{z}_+^2 + (2kh)^2] = 2\kappa\lambda\log\left\{(2kh)^2\left[1 + \frac{(\hat{z}_+/2h)^2}{(2n+1)^2}\right]\right\}. \tag{7}$$

The sum of potentials λ_m and λ_{-m} of images with even m is expressed by the formula

$$\begin{aligned} \mathrm{U}_m &= -2\kappa\lambda\{\log[x - \bar{x} + i(y_- - 2mh)] + \log[x - \bar{x} + i(y_- + 2mh)]\} = \\ &= -2\kappa\lambda\log\left\{(2mh)^2\left[1 + \frac{(\hat{z}_-/2h)^2}{(2n+2)^2}\right]\right\}, \end{aligned} \tag{8}$$

where $\hat{z}_- = x - \bar{x} + iy_-$. The total potential is $\mathrm{U} = \sum_k \mathrm{U}_k + \sum_m \mathrm{U}_m$,

$$\mathrm{U}_{\mathrm{im}}(\hat{z}_+, \hat{z}_-) = 2\kappa\lambda\left[\log\frac{\prod_{n=0}^{\infty}(2n+1)^2}{\prod_{n=0}^{\infty}(2n+2)^2} + \log\prod_{n=0}^{\infty}\left(1 + \frac{(\hat{z}_+/2h)^2}{(2n+1)^2}\right) - \log\prod_{n=0}^{\infty}\left(1 + \frac{(\hat{z}_-/2h)^2}{(2n+2)^2}\right)\right]. \tag{9}$$

The first constant summand does not contribute when the field components are calculated.

The representation of hyperbolic functions as infinite products allows reducing (9) to the form

$$\mathrm{U_{im}}(\hat{z}_+, \hat{z}_-) = 2\kappa\lambda\{\log[\cosh\hat{\delta}_+] - \log[\sinh\hat{\delta}_-] + \log\hat{\delta}_-\}, \tag{10}$$

where $\hat{\delta}_+ = \pi\hat{z}_+/4h$ and $\hat{\delta}_- = \pi\hat{z}_-/4h$.

In the old textbook [11], a similar problem for an electrostatic field of images was solved by the method of conformal maps. Only the potential of the field was calculated. The expression for the potential coincides with (10) if we change $a = 2h$ and $b = h + \bar{y}$ in formula (3) in Sec. 4.20 in [11] and do not use the normalized variables.

We differentiate complex potential (10) with respect to z and obtain the expression for the total complex field of electric images

$$\mathrm{E_{im}}(z) = \frac{2\kappa\lambda}{h}\frac{\pi}{4}\left[\coth(\hat{\delta}_-) - \tanh(\hat{\delta}_+) - \frac{1}{\hat{\delta}_-}\right]. \tag{11}$$

By definition (5), the real components $\mathrm{E}_{x,\mathrm{im}}$ and $\mathrm{E}_{y,\mathrm{im}}$ of the electric field are calculated by the formulas

$$\mathrm{E}_{x,\mathrm{im}} = -\mathrm{Re}\frac{\partial \mathrm{U}}{\partial z}, \qquad \mathrm{E}_{y,\mathrm{im}} = \mathrm{Im}\frac{\partial \mathrm{U}}{\partial z}. \tag{12}$$

We now introduce the normalized coordinates $\delta_x = x/h$ and $\delta_y = y/h$ of the field observation point, the normalized coordinates $\bar{\delta}_x = \bar{x}/h$ and $\bar{\delta}_y = \bar{y}/h$ of the beam position, and the quantities $\Delta_x = \delta_x - \bar{\delta}_x$, $\Delta_{y-} = \delta_y - \bar{\delta}_y$, and $\Delta_{y+} = \delta_y + \bar{\delta}_y$. After simple but lengthy algebraic transformations, we obtain the formulas for the components of the total field of images:

$$\mathrm{E}_{x,\mathrm{im}}(x,y) = \frac{2\kappa\lambda}{h}\frac{\pi}{8}\frac{\sinh(\pi\Delta_x/2)\cos(\pi\delta_y/2)\cos(\pi\bar{\delta_y}/2)}{[\sinh^2(\pi\Delta_x/4) + \cos^2(\pi\Delta_{y+}/4)][\sinh^2(\pi\Delta_x/4) + \sin^2(\pi\Delta_{y-}/4)]} -$$
$$- \frac{2\kappa\lambda}{h}\frac{\Delta_x}{\Delta_x^2 + \Delta_{y-}^2}, \tag{13}$$
$$\mathrm{E}_{y,\mathrm{im}}(x,y) = \frac{2\kappa\lambda}{h}\frac{\pi}{8}\left\{\frac{\sin(\pi\Delta_{y+}/2)}{\sinh^2(\pi\Delta_x/4) + \cos^2(\pi\Delta_{y+}/4)} + \frac{\sin(\pi\Delta_{y-}/2)}{\sinh^2(\pi\Delta_x/4) + \sin^2(\pi\Delta_{y-}/4)}\right\} -$$
$$- \frac{2\kappa\lambda}{h}\frac{\Delta_{y-}}{\Delta_x^2 + \Delta_{y-}^2}. \tag{14}$$

To obtain the total distribution of the electric field between the conducting planes and to satisfy the boundary conditions on the planes, we must sum the image field $\mathbf{E}_{\mathrm{im}}$ and the proper beam field,

$$\mathrm{E}_{x,\mathrm{dir}}(x,y) = \frac{2\kappa\lambda}{h}\frac{\Delta_x}{\Delta_x^2 + \Delta_{y-}^2}, \qquad \mathrm{E}_{y,\mathrm{dir}}(x,y) = \frac{2\kappa\lambda}{h}\frac{\Delta_{y-}}{\Delta_x^2 + \Delta_{y-}^2}. \tag{15}$$

We note several features of expressions (13) and (14). First, the coordinates of the field observation point appear only in the normalized form. Second, the last terms in (13) and (14) have signs opposite to the signs of the components of the (direct) proper field of the beam. Summing (13), (14), and (15) componentwise,

we obtain the components of the total field

$$\mathrm{E}_{x,\mathrm{tot}}(\delta_x,\delta_y,\bar{\delta_x},\bar{\delta_y}) = \frac{2\kappa\lambda}{h}\frac{\pi}{8}\frac{\sinh[\pi(\delta_x-\bar{\delta}_x)/2]}{[\sinh^2[\pi(\delta_x-\bar{\delta}_x)/4]+\cos^2[\pi(\delta_y+\bar{\delta}_y)/4]]}\times$$

$$\times\frac{\cos(\pi\delta_y/2)\cos(\pi\bar{\delta_y}/2)}{[\sinh^2[\pi(\delta_x-\bar{\delta}_x)/4]+\sin^2[\pi(\delta_y-\bar{\delta_y})/4]]}, \tag{16}$$

$$\mathrm{E}_{y,\mathrm{tot}}(\delta_x,\delta_y,\bar{\delta_x},\bar{\delta_y}) = \frac{2\kappa\lambda}{h}\frac{\pi}{8}\biggl\{\frac{\sin[\pi(\delta_y+\bar{\delta_y})/2]}{\sinh^2[\pi(\delta_x-\bar{\delta}_x)/4]+\cos^2[\pi(\delta_y+\bar{\delta_y})/4]}+$$

$$+\frac{\sin[\pi(\delta_y-\bar{\delta_y})/2]}{\sinh^2[\pi(\delta_x-\bar{\delta}_x)/4]+\sin^2[\pi(\delta_y-\bar{\delta_y})/4]}\biggr\}. \tag{17}$$

A direct verification shows that expression (16) satisfies the boundary condition $\mathrm{E}_{x,\mathrm{tot}}(\delta_x,\pm1,\bar{\delta_x},\bar{\delta_y}) = 0$ and $\mathrm{E}_{x,\mathrm{tot}} = 0$ for $\delta_x = \bar{\delta_x} = 0$ in the one-dimensional limit. Expression (17) for $\delta_x = \bar{\delta_x} = 0$ similarly takes form (3) with $\delta = \delta_y$ and $\bar{\delta} = \bar{\delta_y}$.

3. Magnetic fields of image currents

We use the fact that $\mathbf{B} = \mathbf{v}\times\mathbf{E}/c^2$. In the component representation with $\mathrm{v}_x = \mathrm{v}_y = 0$ and $\mathrm{v}_z = \mathrm{v}$ taken into account, we have

$$\mathrm{B}_x = -\frac{\beta\mathrm{E}_y}{c}, \qquad \mathrm{B}_y = \frac{\beta\mathrm{E}_x}{c}. \tag{18}$$

On the surface of a ferromagnet with a very large magnetic permeability ($\mu\to\infty$), only the normal component of $\mathbf{B}$ is nonzero. This boundary condition is satisfied if the image currents have the same direction as the beam current.

Taking the relation between the components of elementary fields $\mathbf{B}$ and $\mathbf{E}$ given by (18) into account, we use the complex potential method as in the preceding section. We place the ferromagnetic planes at distances $y = \pm g$ from the origin. After obvious changes in (7) and (8), we obtain an analogue of expression (10)

$$\widehat{\mathrm{U}}_{\mathrm{im}}(\hat{\eta}_+,\hat{\eta}_-) = -\frac{2\kappa\lambda\beta}{c}\{\log[\cosh\hat{\eta}_+]+\log[\sinh\hat{\eta}_-]-\log\hat{\eta}_-\}, \tag{19}$$

where $\hat{\eta}_+ = \pi\hat{z}_+/4g$ and $\hat{\eta}_- = \pi\hat{z}_-/4g$. For the total complex magnetic induction of image currents, we obtain

$$\mathrm{B}_{\mathrm{im}}(z) = \frac{2\kappa\lambda\beta}{gc}\frac{\pi}{4}\biggl[\tanh\hat{\eta}_+ + \coth\hat{\eta}_- - \frac{1}{\hat{\eta}_-}\biggr]. \tag{20}$$

The components $\mathrm{B}_{x,\mathrm{im}}$ and $\mathrm{B}_{y,\mathrm{im}}$ of the magnetic induction vector are calculated by the formulas $\mathrm{B}_{x,\mathrm{im}} = -\mathrm{Im}\,\partial\widehat{\mathrm{U}}/\partial z$ and $\mathrm{B}_{y,\mathrm{im}} = -\mathrm{Re}\,\partial\widehat{\mathrm{U}}/\partial z$ or directly from (20). To obtain the total distribution of the magnetic field between the ferromagnetic planes and to satisfy the boundary conditions on the planes, we must sum the total field of the image currents $\mathbf{B}_{\mathrm{im}}$ and the proper field of the beam. As previously for the electric field, we sum $\mathrm{B}_{x,\mathrm{im}}$, $\mathrm{B}_{y,\mathrm{im}}$, $\mathrm{B}_{x,\mathrm{dir}}$, and $\mathrm{B}_{y,\mathrm{dir}}$ componentwise and obtain components of the total magnetic induction vector

$$\mathrm{B}_{x,\mathrm{tot}}(\eta_x,\eta_y,\bar{\eta}_x,\bar{\eta}_y) = \frac{\kappa\pi\lambda\beta}{4gc}\biggl\{\frac{\sin[\pi(\eta_y+\bar{\eta}_y)/2]}{\sinh^2[\pi(\eta_x-\bar{\eta}_x)/4]+\cos^2[\pi(\eta_y+\bar{\eta}_y)/4]}-$$

$$-\frac{\sin[\pi(\eta_y-\bar{\eta}_y)/2]}{\sinh^2[\pi(\eta_x-\bar{\eta}_x)/4]+\sin^2[\pi(\eta_y-\bar{\eta}_y)]/4}\biggr\}, \tag{21}$$

$$\mathrm{B}_{y,\mathrm{tot}}(\eta_x,\eta_y,\bar\eta_x,\bar\eta_y)=\frac{\kappa\pi\lambda\beta}{4gc}\biggl\{\frac{\sinh[\pi(\eta_x-\bar\eta_x)/2]}{\sinh^2[\pi(\eta_x-\bar\eta_x)/4]+\cos^2[\pi(\eta_y+\bar\eta_y)/4]}+$$
$$+\frac{\sinh[\pi(\eta_x-\bar\eta_x)/2]}{\sinh^2[\pi(\eta_x-\bar\eta_x)/4]+\sin^2[\pi(\eta_y-\bar\eta_y)/4]}\biggr\},\tag{22}$$

where $\eta_x=x/g$, $\bar\eta_x=\bar x/g$, $\eta_y=y/g$, and $\bar\eta_y=\bar y/g$.

It is difficult to see directly from (21) that the boundary condition $\mathrm{B}_{x,\mathrm{tot}}(\eta_x,\pm1,\bar\eta_x,\bar\eta_y)=0$ is satisfied for $\eta_y=\pm1$. But we can see that $\mathrm{B}_{x,\mathrm{tot}}\sim\cos(\pi\eta_y/2)$, and this boundary condition is therefore indeed satisfied. A direct verification shows that expression (21) takes form (3) at $x=\bar x=0$ with $\eta=\eta_y$ and $\bar\eta=\bar\eta_y$ and that $\mathrm{B}_{y,\mathrm{tot}}=0$ at $x=\bar x=0$.

4. Surface charge density

The distribution of the charge density σ induced by the beam on the conductor surface is determined by the magnitude of the normal component $\mathrm{E_n}$ of the electric field strength at a given point on the surface. In our problem,

$$\mathrm{E_n}=-\mathrm{E}_{y,\mathrm{tot}}(\delta_x,\pm1,\bar\delta_x,\bar\delta_y).$$

The distributions of the charge density σ differ on the upper and lower planes $\delta_y=+1$ and $\delta_y=-1$. Thus, by the Gauss–Ostrogradsky theorem, we have

$$\sigma_{\pm1}(\delta_x,\bar\delta_x,\bar\delta_y)=-\epsilon_0\mathrm{E}_{y,\mathrm{tot}}(\delta_x,\pm1,\bar\delta_x,\bar\delta_y),\tag{23}$$

where $\mathrm{E}_{y,\mathrm{tot}}$ is given by formula (17).

5. Linear approximation for fields

An interesting mathematical feature of the exact functions $\Lambda(\delta,\bar\delta)$ and $H(\eta,\bar\eta)$ in formulas (3) was noted in [2]. This is a kind of permutation symmetry relating the field components $\mathrm{E}_{y,\mathrm{im}}$ and $\mathrm{B}_{x,\mathrm{im}}$. This functional symmetry obviously follows from expressions (4): $H(\eta,\bar\eta)=\Lambda(\bar\eta,\eta)$. For two-dimensional solutions (17) and (21), we can directly verify that the functional parts of the fields preserve this symmetry, which is also present in expressions (2).

A direct derivation of the linear approximation for the field components $\mathbf{E}_{\mathrm{im}}(x,y)$ from relations (16) and (17) is rather laborious. The result can be obtained faster using the complex form of (11). We expand the function of two variables $\mathrm{E}_{\mathrm{im}}(z)$ in a series near the point $(\bar x,\bar y)$ and keep the terms linear in $x-\bar x$ and $y-\bar y$. But expanding $\coth\delta_-$, we must take the singular term $\coth\hat\delta_-\approx\hat\delta_-^{-1}+\hat\delta_-/3+\cdots$ into account. We thus obtain

$$\mathrm{E}_{\mathrm{im}}(z)\approx-\frac{4\kappa\lambda}{h}\biggl\{\epsilon_1(\bar\delta_y)[(\delta_x-\bar\delta_x)+i(\delta_y-\bar\delta_y)]+i\frac{\pi}{8}\tan\biggl(\frac{\pi}{2}\bar\delta_y\biggr)\biggr\}\tag{24}$$

or, in components,

$$\mathrm{E}_{x,\mathrm{im}}\approx-\frac{4\kappa\lambda}{h}\epsilon_1(\bar\delta_y)(\delta_x-\bar\delta_x),\qquad\mathrm{E}_{y,\mathrm{im}}\approx\frac{4\kappa\lambda}{h}\biggl[\frac{\pi}{8}\tan\biggl(\frac{\pi}{2}\bar\delta_y\biggr)+\epsilon_1(\bar\delta_y)(\delta_y-\bar\delta_y)\biggr]\tag{25}$$

by virtue of (5). We here introduce a generalization [2] of the Laslett electric form factor ϵ_1 to the case of an arbitrary vertical beam displacement $\bar\delta_y$,

$$\epsilon_1(\bar\delta_y)=\frac{\pi^2}{32}\biggl[\frac{1}{\cos^2(\pi\bar\delta_y/2)}-\frac{1}{3}\biggr],\qquad\epsilon_1(0)=\frac{\pi^2}{48}.\tag{26}$$

After the one-dimensional problem is solved and $\mathrm{E}_{y,\mathrm{im}}$ of form (2) is determined, to determine the second field component $\mathrm{E}_{x,\mathrm{im}}$, the condition that must be satisfied by components of the fields of images is usually used [12], [1],

$$\boldsymbol{\nabla}\mathbf{E}_{\mathrm{im}} = \frac{\partial \mathrm{E}_{x,\mathrm{im}}}{\partial x} + \frac{\partial \mathrm{E}_{y,\mathrm{im}}}{\partial y} = 0. \tag{27}$$

It is easy to verify that field projections (25) calculated above satisfy condition (27).

We now calculate the components of the magnetic induction vector in the linear approximation. For this, we use complex representation (20). Repeating the expansion of hyperbolic functions in series, just as in calculating E_{im}, we obtain

$$\mathrm{B}_{x,\mathrm{im}} \approx \frac{4\kappa\lambda\beta}{gc}\left[\frac{\pi}{8}\tan\left(\frac{\pi}{2}\bar{\eta}_y\right) + \epsilon_2(\bar{\eta_y})(\eta_y - \bar{\eta}_y)\right], \qquad \mathrm{B}_{y,\mathrm{im}} \approx \frac{4\kappa\lambda\beta}{gc}\epsilon_2(\bar{\eta_y})(\eta_x - \bar{\eta}_x). \tag{28}$$

We here introduce the generalization [2], [13] of the magnetic Laslett form factor ϵ_2 to the case of an arbitrary vertical beam displacement $\bar{\eta}_y$,

$$\epsilon_2(\bar{\eta}_y) = \frac{\pi^2}{32}\left[\frac{1}{\cos^2(\pi\bar{\eta}_y/2)} + \frac{1}{3}\right], \qquad \epsilon_2(0) = \frac{\pi^2}{24}. \tag{29}$$

In conclusion, we note that condition (27) is not a universal method for reconstructing the missing components of the field. Indeed, if we begin with a "wrong" component, for example, if only the component $\mathrm{E}_{x,\mathrm{im}}$ is known, then $\mathrm{E}_{y,\mathrm{im}}$ can be reconstructed only up to an unknown constant C. There are no additional conditions for reconstructing this constant in the form $C = (\pi/8)\tan(\pi\bar{\delta}_y/2)$.

Another applicability constraint of the linear approximation of form (2) or of improved form (25) near the conductor surface is that the boundary condition $\mathrm{E}_{x,\mathrm{tot}} = \mathrm{E}_{x,\mathrm{im}} + \mathrm{E}_{x,\mathrm{dir}} = 0$ is not satisfied for $\delta_y = \pm 1$. The same also concerns the component $\mathrm{B}_{x,\mathrm{im}}$ given by (28): $\mathrm{B}_{x,\mathrm{tot}} \neq 0$ for $\eta_y = \pm 1$.

The permutation symmetry mentioned at the beginning of this section is lost in linear approximations (25) and (28) for exact values of the components $\mathrm{E}_{y,\mathrm{im}}$ and $\mathrm{B}_{x,\mathrm{im}}$.

Acknowledgments. The author thanks E. B. Oborneva for the discussions and support of this project.

Conflicts of interest. The author declares no conflicts of interest.

REFERENCES

1. H. Wiedemann, *Particle Accelerator Physics*, Springer, Berlin (2007).
2. B. B. Levchenko, "Modification of relativistic beam fields under the influence of external conducting and ferromagnetic flat boundaries," *Prog. Theor. Exp. Phys.*, **2020**, 013G01 (2020).
3. W. Thomson, "On electrical images," in: *Notices and Abstracts of Communications to the* 17*th Meeting of the British Association for the Advancement of Science* (Oxford, June 1847), Vol. 1, John Murray, London (1848), pp. 6–7.
4. J. C. Maxwell, "Theory of electric images and electric inversion," in: *A Treatise on Electricity and Magnetism*, Oxford Univ. Press, Oxford (1873), pp. 191–225.
5. L. J. Laslett, "On intensity limitations imposed by transverse space-charge effects in circular particle accelerators," in: *Proc. Summer Study on Storage Rings* (Brookhaven Natl. Lab. Report No. 7534), Brookhaven Natl. Lab., New York (1963), pp. 324–363.
6. A. W. Chao, *Physics of Collective Beam Instabilities in High Energy Accelerators*, John Wiley and Sons, New York (1993).
7. B. B. Levchenko, "Electric and magnetic fields generated by a charged bunch between parallel conducting plates," *Phys. Res. Intern.*, **2010**, 201730 (2010).

8. G. Apollinari, A.I. Béjar Alonso, O. Brüning, P. Fessia, M. Lamont, L. Rossi, and L. Tavian, eds., *High-Luminosity Large Hadron Collider* (*HL-LHC*) *Technical Design Report* V.0.1 (CERN Yellow Reports: Monographs, Vol. 4), CERN Publ., Geneva (2017).
9. B. B. Levchenko, "On field emission in high energy colliders initiated by a relativistic positively charged bunch of particles," arXiv:physics/0608135 (2006).
10. R. Cimino, I. R. Collins, M. A. Furman, M. Pivi, F. Ruggiero, G. Rumolo, and F. Zimmermann, "Can low-energy electrons affect high-energy physics accelerators?" *Phys. Rev. Lett.*, **93**, 014801 (2004).
11. W. R. Smythe, *Static and Dynamic Electricity*, McGraw-Hill, New York (1950).
12. A. Hofmann, "Tune shifts from self-fields and images," in: *Proc. 5th General Accelerator Physics Course* (Jyväskylä, Finland, 7–18 September 1992, S. Turner, ed.,), Vol. 1, CERN Publ., Geneva (1994), pp. 329–348.
13. B. Zotter, "The Q-shift of off-center particle beams in elliptic vacuum chambers," *Nucl. Instrum. Meth.*, **129**, 377–395 (1975).